Plant Cell Biotechnology and Molecular Biology 21(67&68):87-101; 2020 ISSN: 0972-2025

THE PHYSICOCHEMICAL PROPERTIES OF AGRICULTURAL WASTE INOCULATED WITH ALGINATE-PRODUCING BACTERIA: STRUCTURAL MODIFICATION FOR BIOCHAR STABILITY AS A SOIL AMENDMENT FORMULA

SUKMAWATI[*], AMBO ALA, BAHARUDDIN PATANDJENGI AND SIKSTUS GUSLI

Agriculture Study Program, Graduate School, Hasanuddin University, Makassar 90245, Indonesia [Sukmawati].

Faculty of Agriculture, Animal Husbandry, and Fisheries, Universitas Muhammadiyah Parepare, Jenderal ahmad Yani Street 90235 Parepare, South Sulawesi, Indonesia [Sukmawati].

Department of Agrotechnology, Faculty of Agriculture, Hasanuddin University, Makassar 90245, Indonesia [AA].

Department of Plant Pest and Disease, Faculty of Agriculture, Hasanuddin University, Makassar 90245, Indonesia [BP].

Department of Soil Science, Faculty of Agriculture, Hasanuddin University, Makassar 90245, Indonesia [SG].

[*For Correspondence: E-mail: sukmakuuh76@gmail.com]

Article Information

Editor(s):
(1) Dr. Bishun Deo Prasad, Bihar Agricultural University, India.
Reviewers:
(1) Gitanjali Jothiprakash, Tamil Nadu Agricultural University, India.
(2) Valmir Felix de Lima, Federal University of Pernambuco, Brazil.
(3) Maurício Motta, Federal University of Pernambuco, Brazil.

Received: 20 September 2020
Accepted: 25 November 2020
Published: 19 December 2020

Original Research Article

ABSTRACT

This study aims to study the physicochemical characteristics of biochar produced from agricultural waste (palm kernel shells, empty fruit bunches and corn cobs), and its changes after being treated with alginate-producing bacterial isolates. After inoculation of the alginate-producing bacterial isolate coded KK1-40 for 28 days, biochar characterization was carried out which included surface functional groups and biochar structures (porosity and crystal) using FTIR and XRD, respectively. The results showed that the bacterial isolate KK1-40 changed the surface of the biochar by shifting the value of the hydroxyl (O-H) carboxyl (C = O) band, aromatic rings (C = C) and alcohol. Inoculation of bacterial isolates in biochar improved the structure and aromatics of oil palm shell and empty fruit bunches and increased porosity through hexagonal changes and 002 diffraction.From this study, it can be concluded that biochar stabilization in the soil is influenced by alginate-producing bacteria introduced into biochar

products. This study presents a new biochar structure modification through in-situ biopolymer-based activation, so that it is more effectively used as a soil amendment that leads to improved agricultural land.

Keywords: Amorphous; crystallinity; functional groups; polymer; porosity.

ABBREVIATIONS

CEC= Cation Exchanges Capability;
FITR= Fourier transform infrared spectroscopy;
XRD= X-Ray Diffraction.

INTRODUCTION

A new era of agricultural environmental management based on various studies has revealed the use of biochar as a sustainable approach in improving soil quality [1]. Among the mechanisms involved with biochar use are increased soil aeration and water holding capacity, increased microbial activity and nutrient status in the soil, and changes in some important soil chemical properties [2]. As a soil amendment agent, biochar must have high binding capacity so that it does not have a negative impact on soil structure [3].

Biochar is generally made from agricultural waste such as leftover oil palm or corn which is widely available. The huge potential of biochar raw material provides opportunities for land improvement, especially in dry land, by taking into account the potential role of biochar associated with its ability to increase water and nutrient retention. Physical characteristics of biochar, such as surface area, shape, structure and porosity, play an important role in groundwater retention [4,5], nutrient retention and aeration [6].

Biochar has an influence on microbial abundance [7]. Biochar pores play an important role as habitat protection and are used as a carbon source. Thus, it can support the microbial population and its activities in the soil [8]. An increase in microbial abundance occurs after being absorbed onto the biochar surface, through hydrophobic attraction, electrostatic forces and the formation of deposits [9]. The level of microbial attachment is determined by the surface area of the biochar, while the pore structure is a shelter for soil microbes [10].

Several physical properties of soil, such as the distribution of soil aggregates, are directly related to bacteria. Soil aggregation requires adhesive compounds, namely polysaccharides [11], which are secreted by bacteria. Alginate is an important component of exopolysaccharide [12] which helps bacteria to overcome water pressure [13]. This group of bacteria is known to have hydrophilic properties that are able to bind water and have a negative charge which in turn will affect the potential for groundwater [14] are resistant to drought and become a binding agent for nutrients through chemical reactions [15].

Although many studies have reported the effect of biochar in increasing plant growth, the use of biochar that has been enriched by microbes, both bacteria and fungi, is still lacking [16,17]. Nevertheless, the study of Tu et al. [18] have demonstrated the potential use of biochar with bacterial loads to improve soil physical and chemical properties in stabilizing heavy metals in contaminated soils. In addition, previous research has also shown the important role of biochar and alginate-producing bacteria in the efficiency of water and nutrient use during the growth of maize [19].

Microbial inoculants can recycle and increase the efficiency of nutrient use in agricultural land, thereby regulating soil and crop fertility. Thus it can reduce abiotic stress in plants [20]. The symbiotic relationship with microbes occurs through the availability of nutrients formed from various plant needs, such as increased carbon supply with root exudation in the rhizosphere, where carbon is a source of energy for heterotropic microorganisms [7]. The diversity of microbes with their various activities plays a role in efficient nutrient transfer to plants and greater nutrient retention in the soil [21].

Despite this, bacteria that colonize the surface of the biochar can modify the physicochemical characteristics of the biochar through degradation of the organic matter. Therefore, physicochemical

characterization is a key factor in biochar production and enrichment with bacteria as a soil amendment to improve soil properties [21]. The addition of bacteria such as alginate-producing bacteria allows interactions that support microbial growth [22]. However, investigations into the nature of the interactions between biochar and bacteria are needed to understand the possible changes in the psychochemical properties of biochar. Therefore, this research is aimed at increasing the stability of biochar related to its use as an efficient soil repairing formula for agricultural land improvement, through the addition of alginate-producing bacteria.

MATERIALS AND METHODS

Biochar and Alginate-producing Bacteria Isolate Preparation

Biochar raw materials are derived from oil palm shells, oil palm empty fruit bunches and corncobs, which were burned using tools and procedures that are easily adopted by farmers. All three types of biomass were dried under the sun for three days then burnt using a gas stove [23] for 4 hours with a temperature range between 300°C-400°C [24]. After chilling, biochar were mashed using a blender [25], then sieved using a 0.250 mm size sieve.

For each type of biochar, 10 g of biochar (pH 7.54, 60% humidity) is placed in a glass bottle then covered with aluminum foil and plastic. The bottles are then put into an autoclave to be sterilized for 45 minutes at a temperature of 121°C. After cooling, bacterial isolates (0.5 ml with a density of 10^9 CFU / ml) were injected into the biochar medium. The incubation process lasts for 28 days at 28°C. The alginate-producing bacteria isolate with code KK1-40 is a private collection, isolated from the cocoa rhizosphere and has been analyzed for identification.

Fourier Transform Infrared Spectroscopy (FTIR) Analysis

Fourier transform infrared spectroscopy (FTIR) analysis was performed by referring to the procedure of [26,27]. Whereas FTIR spectrum interpretation [28,29,30,31,32], referred to: hydroxyl acid O-H (300-3690 cm^{-1}), alkane CH (2927-2856 cm^{-1},1446-1370 cm^{-1}), aromatic ring C = C (1560-1600 cm^{-1}), carboxylic acid C = O (1560 -1600 cm^{-1}), C-OH (1033 cm^{-1}). The FTIR spectroscopy was performed on an IRPrestige-21 FT-IR (Shimadzu Corp) spectrometer, equipped with a bright ceramic light source, KBr beamsplitter, and tri-glycine sulfate doped with L-alanine (DLATGS). Sample measurements were collected in the range of 4000-600 cm^{-1} and 16 additional scans. All FTIR spectra are in the transmittance unit. For magnetic studies the sample used a vibrating magnetometer (Oxford Instruments, VSM 1.2 H).

X-Ray Diffraction Analysis

Spectra were collected in XRD spectroscopy (Shimidzu 7000). X-ray diffractometers are equipped with Cu-Ka Ni-filtered radiation (k = 1,5406 Å) at an acceleration voltage of 40 kV and an emission current of 40 mA to direct X-rays in the sample. The range of X-ray diffraction patterns was set from 10° to 70°. The analysis was carried out for 30 minutes at 2.5°/ minutes. The composition of sample elements was determined by X-sinate spectroscopy (XRF, Thermo ARL QANT'X EDXRF models) [33]. This analysis observed the biochar structure and porosity following method of Tahir et al. [34], using the Deby-Scherrer equation:

$$D = \frac{K\lambda}{\beta \cos \theta}$$

Where: D = crystal size, λ = wave XRD, β = FWHM (Full Width Half Maximum, θ = large angle from the highest peak intensity.

$$\delta = \frac{1}{D^2}$$

The lattice parameter for the hexagonal structure a = b ≠ c is determined from the equation:

$$\frac{1}{d^2} = \frac{4}{3}\left(\frac{h^2hk + k^2}{a^2}\right) + \frac{l^2}{c^2}$$

X-ray density (ρs), biochar density (pb), and porosity (P) of biochar and biochar after adding

alginate-producing bacterial isolates were determined using the equation, respectively.

$$\rho_s \frac{nM}{N_{ac}} = \frac{nM}{NV_{cal}}$$

$$\rho_b \frac{m}{V_b}$$

Where: n = 4, the number of molecules for carbon for composites, is a weighted average value for the number of molecules per unit of carbon of the biochar and the bacteria loaded biochar. M = molecular weight (carbon), N is Avogadro's number (6.019 x 10^{23}) a and c are lattice parameters from XRD Spectra analysis, and Vcl = is the unit cell volume calculated from lattice parameters. Biochar density was calculated using the biochar mass (m) used 0.15 g and volume (Vb) = 0.489 determined from the analyzed biochar sample.

$$P = \left(1 - \frac{\rho_b}{\rho_s}\right) x\, 100\%$$

where: ρ_s = X-ray density, P = porosity (%), ρ_b = biochar density.

Data Analysis

Data from XRD analysis were plotted using Matlab 2013b program to obtain the XRD spectrum graph for biochar structures for further interpretation.

RESULTS AND DISCUSSION

Biochar Surface Functional Groups

Table 1 shows the biochar FTIR spectra of the oil palm shells, oil palm empty fruit bunches and corncobs biochar produced with pyrolysis temperature ranged 300-400°C. Hydroxyl (O-H) bonds spectra appear on all biochar surfaces on the broad band on 3200-3600 cm^{-1}. However, the results of the spectra showed that the addition of alginate-producing bacterial isolates resulted in a shift in the wave number with a wider band (Fig. 1). The FTIR spectrum pattern of biochar absorption from oil palm shells, oil palm empty bunches and corn cobs changed after adding alginate-producing bacterial isolates (KK1-40), with an incubation period of 28 days at 28oC. The change in spectrum in the form of shifted absorption is shown by FTIR spectra. KK1-40 bacterial isolates were able to shift the alcohol absorption band (C-O) to be smaller (1020.34 cm-1 and 1022.27 cm-1). This has an effect on the absorption of the hydroxyl acid (O-H) functional groups, where there is a shift in the value to low, respectively from 3442.9 cm-1 to 3421.72 cm-1 and 3415.93 cm^{-1}. Another case with the absorption of the carboxyl acid functional group (C = O), it actually experienced a bigger shift in value accompanied by an increase in absorption intensity from the 1612.49 cm-1 band to 1701.22 cm-1; 1693.5 cm-1; 1693, 5 cm-1. Likewise, the aromatic ring functional group (C = C) experienced a larger value shift accompanied by an increase in absorption intensity (from the band 1512.19 cm-1, to 1585.49 cm-1; 1591.27 cm-1 and 1597.06. cm-1). There was no change in the carbon framework, where there was no shift in the value of the alkane functional groups in the 2922.16 cm-1 band. The addition of bacterial isolates resulted in a shift in the absorption band of the biochar surface functional groups of oil palm empty bunches, towards a lower value in the fingerprint area. This occurs in alcohol (OH), from 1033.85 cm-1 to 1024.2 cm-1, as well as the alkane band (CH) (from 1377.17 cm-1 to 1371.39 cm-1; 1369.46 cm-1; 1367.53 cm-1. On the other hand, there was a shift in the aromatic ring band towards a greater value (from the band 1570.06 cm-1 to 1577.77 cm-1 and 1573.91 cm-1). carboxyl, alkanes and hydroxyl acids do not experience a shift in the value of the functional groups.On the other hand, there was a change in functional group changes on the surface of the corncob biochar (Fig. 1). Changes occurred in alcohol (O-H) by shifting the band values to be lower (from 1163.08 cm-1 to 1022.27 cm-1; 1028.06 cm-1 and 1022.27 cm-1). This affects the shift of the hydroxyl band with a lower band value. In addition, there is a shift in the band value to be lower in the aromatic rings and carboxyl acids. However, there is no change in the functional groups in the alkanes. This means that bacterial isolates only use volatile substances as an energy source and do not use bound carbon.

Table 1. Fourier transforms infrared (FTIR) spectra of surface functional groups for three types of agricultural-waste biochar and following inoculation with alginate-producing bacterial isolates for 28 days at 28°C

Biochar	Alcohol (C-O)	Alkanes (C-H)	Aromatic (C = C)	Carboxylic Acid (C = O)	Alkanes (C-H)	Hydroxyl acid (O-H)
1. Biochar						
Oil palm shells	1105	1456	1512	1695	2922	3443
Oil palm empty fruit bunches	1033	1377	1570	1695	2922	3416
Corncobs	1163	1456	1595	1697	2920	3447
2. Biochar +alginate-producing bacterial isolates						
Oil palm shells	1020	1456	1585	1701	2922	3422
Oil palm empty fruit bunches	1024	1454	1578	1697	2922	3418
Corncobs	1022	1456	1566	1690	2920	3418

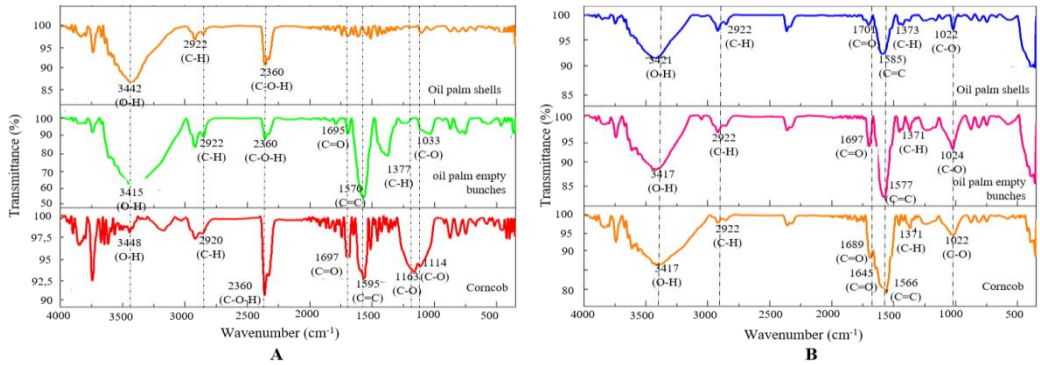

Fig. 1. A.FTIR spectrum of biochar surface functional groups of (oil palm shells, oil palm empty fruit bunches, corncobs) at pyrolysis temperatures of 300-400°C. B. FTIR spectrum of biochar surface functional groups (oil palm shells, palm oil palm bunches and corncobs) after inoculated with alginate-producing bacteria (KK1-40) incubation for 28 daysat 28°C

Characterization of the Biochar Structure

Pyrolysis biochar at a temperature range of 300-400ºC resulted in the highest level of porosity in oil palm empty fruit bunches biochar of 94.84% with a volume of 13.44 and lattice parameters a = 2.16 and c = 7.365 (1 = 10-8 cm) compared to corn cobs biochar (94.31%) and palm kernel shell biochar (92.70) (Table 2). However, after adding KK1-40 bacterial isolates, the porosity changed. We found an increase in porosity of 1.68% in the palm kernel shell biochar. However, there was a decrease in porosity of 2.77% in corncob biochar and 0.053% in oil palm empty bunches biochar. The porosity of the biochar changes due to the lattice parameter that changes the hexagonal volume. Large changes occur in the distance of the graphene sheets indicated by the value of c which changes the matrix to be shorter for each biochar. In addition, there was a widening of the matrix in empty fruit bunches and corn cobs. On the other hand, there was a narrowing of the palm kernel shell biochar (value a).

The results of the spectra show that there isa shift in the peaks of all biochar types due to the addition of isolates KK1-40. The strongest peak of oil palm shell biochar at 22.62°; 23.56°; 21.76° (002) has shifted to 23.2°; 24.42° and 26.66°. Likewise, the strongest peak of oil palm empty bunches biochar at 44.07°; 37.83° and 39.54° (100) to 23.32°; 24.96° and 44.03°. Meanwhile, the strongest peak of corncob biochar was at 44.07°; 37.83° and 39.54° (100), experiencing a peak shift to 24.24°; 25.56°; 25.84° (200) (Fig. 2). The reflection peak of 2θ = 20°-30° ignores the aromatic layer arrangement [35] where the reflection of graphite crystals shows carbon atoms in hexagonal-shaped layers.This causes a crystallinity change in biochar.

Table 2. Lattice parameters, hexagonal volumes and biochar porosity (oil palm shells, oil palm empty fruit bunches, corncobs) pyrolysis at 300-400°C and following inoculation with alginate-producing bacterial isolates for 28 days at 28°C

Biochar	Lattice parameter (Å)		Hexagonal volume	Porosity (%)
	a	c		
1. Biochar results from pyrolysis at a temperature of 300-400°C				
▪ Palm shells	2.36	7.92	19.02	92.70
▪ Oil palm empty fruit bunches	2.16	7.37	13.44	94.84
▪ Corncob	2.15	7.90	14.81	94.31
2. Biochar +alginate-producing bacterial isolates				
▪ Palm shells	2.24	7.25	14.95	94.26
▪ Oil palm empty fruit bunches	2.25	7.25	13.54	94.79
▪ Corncob	2.73	6.72	21.64	91.69

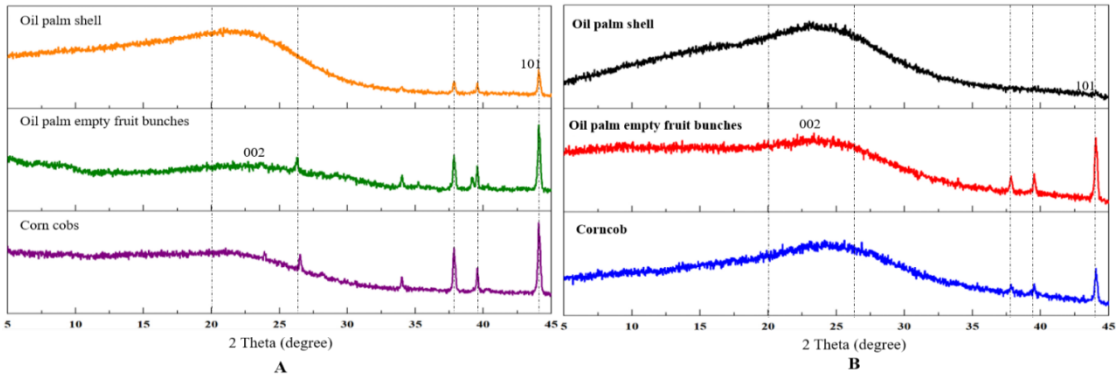

Fig. 2. A.XRD spectrum of biochar structures (oil palm shells, oil palm empty fruit bunches, corncobs) at pyrolysis temperatures of 300-400ºC, B. XRD spectrum of biochar structures (oil palm shells, palm oil palm bunches and corncobs) following inoculation with alginate-producing bacterial isolates for 28 days at 28°C

Carbonization results from the three types of raw materials, namely oil palm shells, oil palm empty fruit bunches and corn cobs, produced crystallization in the form of amorphous and crystals with different ratios (Fig. 3 and Fig. 4). The incorporation of bacteria into the biochar reduced the amorphous area of the oil palm shell from 88.37% to 82.96%. On the other hand, the area of oil palm empty fruit bunches biochar actually increased from 82.06% to 85.97%. Likewise for corncob biochar, increased from 79.30% to 82.96% (Fig. 3B). The carbon peaks of the amorphous structure are regularly reflected by the 002 diffraction peaks. The 002 band reflects the height of the arrangement of the aromatic layer, which is related to the crust formed by the condensation of poly from the aromatic core, aromatic crystals. The diffraction peak of 100 reflects the level of aromatic ring condensation, which concerns the size and layer of the aromatic [36]. The biochar aromatic structure has various forms including amorphous C which is dominant in low pyrolysis which determines biochar stability [37].

Discussion

The effect of combining biochar with alginate-producing bacteria is expected to increase the stability of biochar so that its joint application as a soil enhancer can increase the ability of the soil to hold water and nutrients. The preformation of initial synthesis of the functional groups and biochar structure to determine changes in the surface conditions of the biochar after the alginate-producing bacteria were added. This

condition is crucial, because biochar can change the physicochemical properties of soil and is resistant to microbial decomposition [38]. On the other hand, microbes can change the environment by consuming resources and eliminating metabolites of the biochar [39].

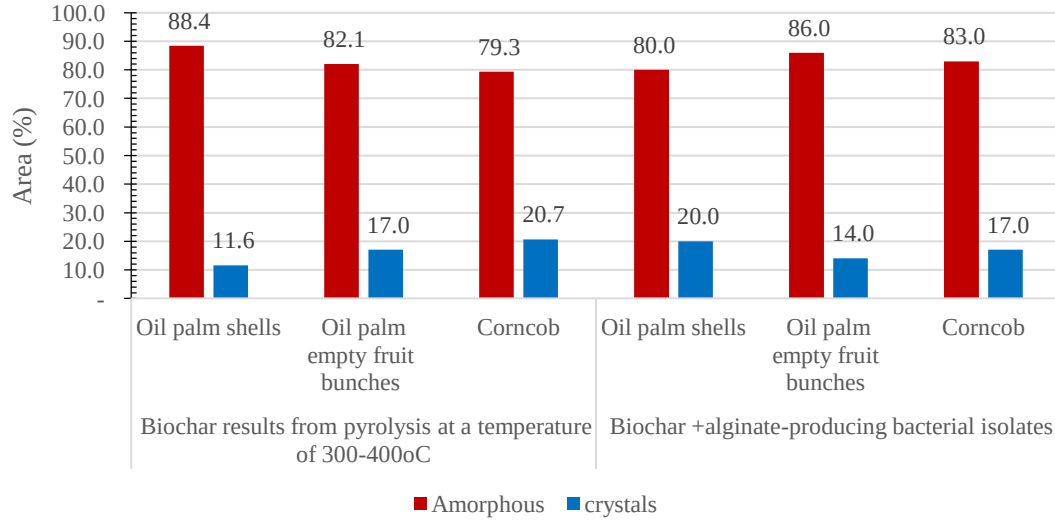

Fig. 3. Biochar crystallization (oil palm shells, oil palm empty fruit bunches, corncobs) at pyrolysis temperature of 300-400°C and following inoculation with alginate-producing bacterial isolates for 28 days at 28°C.

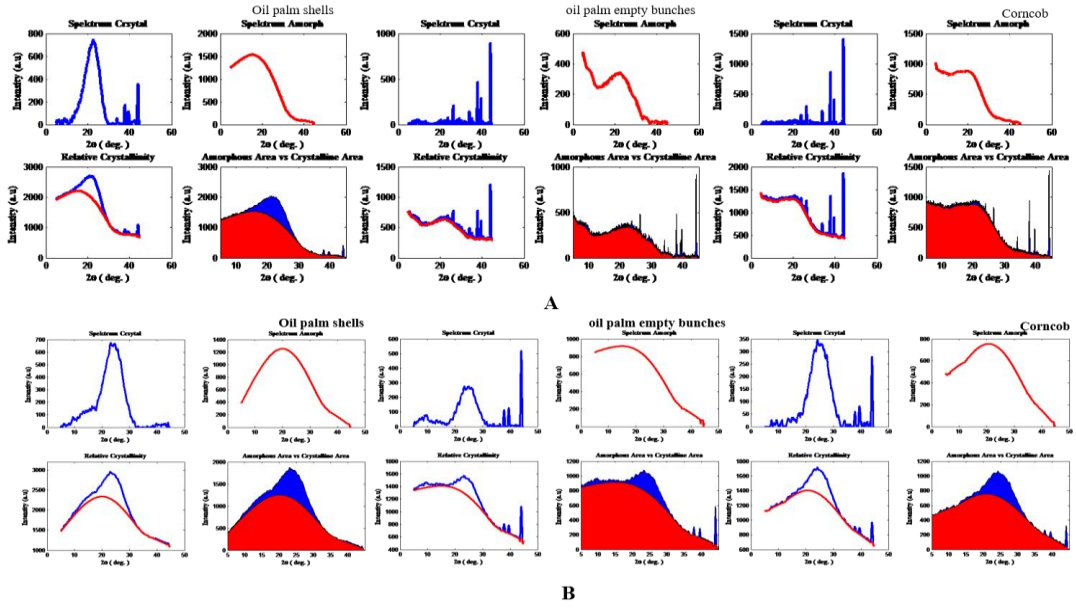

Fig. 4. Comparison of crystal area and amorphous biochar A. pyrolysis temperature 300-400 oC B. After adding alginate-producing bacterial isolates (KK1-40) (black is defined as crystal area and gray as amorphous area)

The changes in surface functional groups in biochar are occured. This shift is clearly seen in corncob biochar. A shift from wave number 3447 cm^{-1} to 3418 cm^{-1} was detected. In addition, the emergence of absorption of the alcohol functional groups, was detected at wave numbers between 1000 and 1300 cm^{-1}, shows that hydroxyl acids were formed into primary alcohols (ethanol). Biochar from oil palm parts biomass (shells and empty fruit bunches), produced a carbon skeleton that is not affected by the activity of the alginate-producing bacteria, was characterized by alkane functional groups that did not experience changes in wave numbers 2922 cm^{-1} and was differed with corncob biochar (2920-2922 cm^{-1}). This can be seen after the addition of alginate-producing bacterial isolates, the wave number did not undergo regeneration. On the contrary in the corn cobs biochar, a shift was observed (2862 cm^{-1} to 2920 cm^{-1}). Nonetheless the carbon skeleton bond between each biochar is still weak, characterized by the alkane group on the stretching band 1340-1470 cm^{-1} with a weak intensity.

The activity of alginate-producing bacteria changed the structure of the biochar carbon to be more aromatic for oil palm shell and oil palm empty fruit bunches biochars, but reduced aromatic properties in the corncobs biochar. This is indicated by an increase in intensity and shift in the value of the carboxyl group (C = O) spectra. This spectrum values increased in the biochar from oil palm shells (1512-1585 cm^{-1}) and oil palm empty fruit bunches (1570-1578 cm^{-1}), but decreased in the corncobs biochar (1595-1566 cm^{-1}). The stretching band of wave numbers from 1600 cm^{-1} to 1800 cm^{-1}, reflecting the functional groups of carboxyl acids, appears on all three biochar surfaces. Bacterial activity is also seen in the shifting of the wave number in the carbonic acid functional groups. This means that during the incubation process, bacteria utilize carbon sources from biochar (See comparison of Fig. 1A with Fig. 1B).

The results of changes in the biochar surface functional group spectra found in the recent study are similar to the results of the research of [40], which found a stretch of the hydroxyl acid and carboxyl acid in the biochar oil palm empty fruit bunches, from 3300 cm^{-1} to 1516 cm^{-1} and 1560 cm^{-1}, respectively. Whereas Liu et al. [41], reported a hydroxyl acid spectra of corncobs biochar on the 3408 cm^{-1} band and the aromatic ring at 1429-1601 cm^{-1}. Aromatic skeletal vibrations (C = O), found at 1597cm^{-1} vibration stretch (Su et al., 2017), are characteristic bands of lignin [29].

The carbon framework shown by wave numbers of 2700-3000 cm^{-1} is an absorption characteristic for alkane groups [31,32], while wave numbers of 1340-1470 cm^{-1} are alkane groups with strong intensity supporting the absorption of alkane groups of wave number 2850-2950 cm^{-1}. The alkane function group is an aliphatic structure that dominates the formation of primary pores together with the oxygen functional group [42]. This relates to the formation of carbon frameworks by alkane functional groups. Pyrolysis temperatures of 300-400°C produce more diverse organic characteristics, due to the formation of aliphatic (alkane) and cellulose structures [43,44]. Based on this, we can speculate that the biochar produced in this study has the structure of carbohydrate cellulose and hemicellulose. This is confirmed by the study of Ghani et al., [45], that the band of 1600-1800 cm^{-1} reflected the hydrocarbon functional groups that can be attributed to the carbohydrate cellulose and hemicellulose structures. The physical of hemicellulose and cellulose decomposed at pyrolysis temperature of 200-500°C [46]. Alkali condition of the biomass promotes the formation of oxygen-containing surface groups [47,48] such as carbonic functional groups. The presence of oxygen-based organic compounds on the surface of biochar significantly influences the cation exchange capacity [49]. Whereas high aromaticity or aromatic condensation levels are useful indicators of biochar structure [50]. The aromatic ring is an aliphatic compound that functions as a bridge connecting the layers of carbon to form a twisted network of carbon structures [51]. The basic concept of biochar as a means of carbon sequestration is shown by the high organic C levels stored in condensed aromatic rings [52]. Biochar which has aromatic characteristics has high stability so that it rejects biological and termochemical degradation [53], so that aromatics in biochar can indicate biotic and abiotic degradation of the biochar in soil [54].

Synthesis of functional group changes shows a shift in spectrum and intensity bands. This confirms that during the incubation process, bacteria use the material present in biochar as a source of food and energy, but will not change the shape of the carbon skeleton. This is reflected in the alkane functional groups that do not change in the palm kernel shell biochar and the empty palm fruit bunch biochar. Meanwhile, for corn cobs biochar, an improvement in the carbon framework was observed which reduced porosity. This is confirmed by the size of the lattice parameter which increases the width of a = 2.15 to 2.73, while the hexagonal height decreases from 7.90 to 6.72, this can be expected if there is a collapse in the carbon framework.

The degree of condensation of the aromatic ring concerns the size and aromatic layer characterized by a peak of 100 (graphite crystal reflection), carbon atoms in a hexagonal layer [35] and a peak of 002 (attribute reflection), reflecting the height of the aromatic layer arrangement, which is associated with crystals formed by polycondensation of aromatic nuclei, namely aromatic crystals [55,56]. Biochar particles consist of two main structural fractions, namely stacked crystalline graphene sheets and random amorphous aromatic structures [57]. The number of aromatic layers has a great influence on the macropore and micropore structures, which easily form between the aromatic layer and the edge of the aromatic structure [58].

Synthesis of functional group changes shows a shift in spectrum and intensity bands. This confirms that during the incubation process, bacteria use the material present in biochar as a source of food and energy, but will not change the shape of the carbon skeleton. This is reflected in the alkane functional groups that do not change in the palm kernel shell biochar and the empty palm fruit bunch biochar. Meanwhile, for corn cobs biochar, an improvement in the carbon framework was observed which reduced porosity This is confirmed by the size of the lattice parameter which increases the width of a = 2.15 to 2.73, while the hexagonal height decreases from 7.90 to 6.72, this can be expected if there is a collapse in the carbon framework.

Crystallinity is affected by the reduced distance between the aromatic layer (Lc = 002) and the narrowing of the aromatic layer (La). This change causes the low level of order (amorphous) to become more regular (crystal) [59], The significant difference between the amorphous region and the crystal region indicates that the biochar in the results of this study has an unstable carbon structure. The conversion of amorphous carbon to crystalline carbon increases the number of micropores. This occurs due to the loss of aliphatic and volatile components, thereby increasing pore volume and surface area [60,56].

Biochar pores play an important role as a protective habitat for microbes, as well as a source of carbon for nutrition. Like in the oil palm shells, with low moisture, it forces bacteria to release polymeric products such as alginate into biofilms to help them deal with drought. Bacteria release alginate with the aim of forming thick structured biofilms and cyst formation to survive drought [61]. The resulting alginate is attached to the surface of the biochar, because organic alginate increases the number of pores on the biochar surface. This is confirmed by the addition of several peaks in the palm oil spectrum of palm oil, such as carbonic acid, which reflects the addition of carbon. In addition, bacteria need energy by utilizing carbon which can be degraded from biochar. The biocar mineralization or oxidation itself is affected by changes in microbial properties. However, this process depends on several aspects, including the amount of available C sources, absorption of organic C, easy degradation, biochar bioactive that exists, or their effects on pH and phenolic substances in microbial communities [62,63]. This is reflected in the top of the aromatic ring which is almost lost in the palm kernel shell biochar. Thus, it can be assumed that during the alginate secretion process for biofilms and cysts for dryness, bacteria use the volatile materials found in biochar as a food source, so that biochar becomes more aromatic, because the pores are cleaner than volatile materials. This synthesis initiates the incorporation of biochar with alginate-producing bacteria as a soil amendment to increase water and nutrient retention.

CONCLUSION

It can be concluded that the inoculation of alginate-producing bacterial isolates into biochar changes its chemical properties in the form of a shift in surface functional groups which leads to the utilization of resources as volatile substances. This causes a change in hexagonal volume and diffraction of 002, so that the porosity increases and is more aromatic. Thus, the possibility of biochar stabilization in the soil is influenced by alginate-producing bacteria. Therefore this research found a new way to activate biochar in situ using alginate-producing bacteria. This provides new hope for the improvement of agricultural land through the addition of carbon-based organic materials and natural polymers such as alginates.

DISCLAIMER

The products used for this research are commonly and predominantly use products in our area of research and country. There is absolutely no conflict of interest between the authors and producers of the products because we do not intend to use these products as an avenue for any litigation but for the advancement of knowledge. Also, the research was not funded by the producing company rather it was funded by personal efforts of the authors.

ACKNOWLEDGEMENTS

Bacteria were kindly provided by the Biotechnology Laboratorium, Hasanuddin University. Raw materials for oil palm plants biochar were obtained from PT. Perkebunan Nusantara XIV. Proximate analysis was assisted by the Mineral and Analysis and Processing Laboratory, Faculty of Engineering, Hasanuddin University. The FITR and XRD analysis was assisted by the Organic Chemistry Laboratory and the Physics Laboratory, Faculty of Mathematics and Science, Hasanuddin University. This research was funded by the Ministry of Research, Technology and Higher Education through the Indonesian Endowment Fund for Education - LPDP).

COMPETING INTERESTS

Authors have declared that no competing interests exist.

REFERENCES

1. Rawat J, Saxena J, Sanwal P. Biochar : A sustainable approach for improving plant growth and soil properties; 2019. Available:https://doi.org/ DOI: 10.5772/intechopen.82151
2. Laghari M, Naidu R, Xiao B, Hu Z, Mirjat MS, Hu M, Kandhro MN, Chen Z, Guo D, Jogi Q, Abudi ZN, Fazal S. Recent developments in biochar as an effective tool for agricultural soil management: A review. Journal of the Science of Food and Agriculture. 2016;96(15):4840–4849. Available:https://doi.org/10.1002/jsfa.7753
3. Lahori AH, Zhanyu GUO, Zengqiang Z, Ronghua LI, Mahar A. Use of biochar as an amendment for remediation of heavy metal-contaminated soils : Prospects and challenges. Pedosphere: An International Journal. 2017;27(6):991–1014. Available:https://doi.org/10.1016/S1002-0160(17)60490-9
4. Andrenelli MC, Maienza A, Genesio L, Miglietta F, Pellegrini S, Vaccari FP, Vignozzi N. Field application of pelletized biochar : Short term effect on the hydrological properties of a silty clay loam soil. Agricultural Water Management. 2016;163:190–196. Available:https://doi.org/10.1016/j.agwat.2015.09.017
5. Liu G, Chen L, Jiang Z, Zheng H, Dai Y, Luo X, Wang Z. Science of the total environment aging impacts of low molecular weight organic acids (LMWOAs) on furfural production residue-derived biochars : Porosity , functional properties , and inorganic minerals. Science of the Total Environment. 2017;607–608: 1428–1436. Available:https://doi.org/10.1016/j.scitotenv.2017.07.046
6. Githinji L. Effect of biochar application rate on soil physical and hydraulic properties of a sandy loam. Archives of

Agronomy and Soil Science. 2014;60(4): 457–470.
Available:https://doi.org/10.1080/03650340.2013.821698

7. Lehmann J, Rillig MC, Thies J, Masiello CA, Hockaday WC, Crowley D. Biochar effects on soil biota - A review. Soil Biology and Biochemistry. 2011;43(9): 1812–1836.
Available:https://doi.org/10.1016/j.soilbio.2011.04.022
8. Kolb SE, Fermanich KJ, Dornbush ME. Effect of charcoal quantity on microbial biomass and activity in temperate soils. Soil Science Society of America Journal. 2009;73(4):1173–1181.
Available:https://doi.org/10.2136/sssaj2008.0232
9. George N, Davies JT. Parameters Affecting adsorption of microorganisms on activated charcoal cloth; 1988.
10. Jaafar NM, Clode PL, Abbott LK. Soil Microbial Responses to Biochars Varying in Particle Size, Surface and Pore Properties. Pedosphere. 2015;25(5):770–780.
Available:https://doi.org/10.1016/S1002-0160(15)30058-8
11. Mengistu AG, Mavimbela SSW, van Rensburg LD. Characterisation of the soil pore system in relation to its hydraulic functions in two South African aeolian soil groups. South African Journal of Plant and Soil. 2019;36(2):107–116.
Available:https://doi.org/10.1080/02571862.2018.1487594
12. Chang WS, Van De Mortel M., Nielsen L, De Guzman GN, Li X, Halverson LJ. Alginate production by Pseudomonas putida creates a hydrated microenvironment and contributes to biofilm architecture and stress tolerance under water-limiting conditions. Journal of Bacteriology. 2007; 189(22):8290–8299.
Available:https://doi.org/10.1128/JB.00727-07
13. Ngumbi E, Kloepper J. Bacterial-mediated drought tolerance: Current and future prospects. Applied Soil Ecology. 2016;105: 109–125.
Available:https://doi.org/10.1016/j.apsoil.2016.04.009
14. Nasser A. Mingelgrin U, Gerstl Z. Effect of soil moisture on the release of alachlor from alginate-based controlled-release formulations. 2008;1322–1327.
Available:https://doi.org/doi: 10.1021/jf0718392
15. Costa OYA, Raaijmakers JM, Kuramae EE. Microbial extracellular polymeric substances: Ecological function and impact on soil aggregation. Frontiers in Microbiology. 2018;9:1–14.
Available:https://doi.org/10.3389/fmicb.2018.01636
16. Hale L, Luth M, Kenney R, Crowley D. Evaluation of pinewood biochar as a carrier of bacterial strain Enterobacter cloacae UW5 for soil inoculation. Applied Soil Ecology. 2014;84:192–199.
Available:https://doi.org/10.1016/j.apsoil.2014.08.001
17. He S, Zhong L, Duan J, Feng Y, Yang B, Yang L. Bioremediation of wastewater by iron Oxide-Biochar nanocomposites loaded with photosynthetic bacteria. Frontiers in Microbiology. 2017;8:1–10.
Available:https://doi.org/10.3389/fmicb.2017.00823
18. Tu C, Wei J, Guan F, Liu Y, Sun Y, Luo Y. Biochar and bacteria inoculated biochar enhanced Cd and Cu immobilization and enzymatic activity in a polluted soil. Environment International. 2020;137 105576.
Available:https://doi.org/10.1016/j.envint.2020.105576
19. Sukmawati Ala A, Baharuddin, Gusli S. Biochar interventions enriched with alginate-producing bacteria support the growth of maize in degraded soils Biochar interventions enriched with alginate-producing bacteria support the growth of maize in degraded soils. 2020;0–10.
Available:https://doi.org/10.1088/1755-1315/486/1/012133
20. Sahu PK, Singh DP, Prabha R, Meena KK, Abhilash PC. Connecting microbial capabilities with the soil and plant health: Options for agricultural sustainability. Ecological Indicators, 2019;105:601–612.

Available:https://doi.org/10.1016/j.ecolind.2018.05.084

21. Gul S, Whalen JK, Thomas BW, Sachdeva V, Deng H. Physico-chemical properties and microbial responses in biochar-amended soils: Mechanisms and future directions. Agriculture, Ecosystems and Environment. 2015;206:46–59. Available:https://doi.org/10.1016/j.agee.2015.03.015
22. Sanchez-Monedero MA, Cayuela ML, Roig A, Jindo K, Mondini C, Bolan N. Role of biochar as an additive in organic waste composting. Bioresource Technology. 2018;247:1155–1164. Available:https://doi.org/10.1016/j.biortech.2017.09.193
23. Brown TR, Wright MM, Brown RC. Estimating profi tability of two biochar production scenarios : Slow pyrolysis vs fast pyrolysis. Table. 2011;1:54–68. Available:https://doi.org/10.1002/bbb
24. Hossain MK, Strezov V, Chan KY, Ziolkowski A, Nelson PF. In fl uence of pyrolysis temperature on production and nutrient properties of wastewater sludge biochar. Journal of Environmental Management, 2011;92(1):223–228. Available:https://doi.org/10.1016/j.jenvman.2010.09.008
25. Rasa K, Heikkinen J, Hannula M, Arstila K, Kulju S. Biomass and Bioenergy How and why does willow biochar increase a clay soil water retention capacity ? Biomass and Bioenergy. 2018;119:346–353. Available:https://doi.org/10.1016/j.biombioe.2018.10.004
26. Domingues RR, Trugilho PF, Silva CA, AICN, Melo CA, Magriotis, ZM, Sa MA, Melo D. Properties of biochar derived from wood and high-nutrient biomasses with the aim of agronomic and environmental benefits. 2017;1–19.
27. Tahir D, Ilyas S, Abdullah B, Armynah B, Jae H. Journal of electron spectroscopy and electronic properties of composite iron (II , III) oxide (Fe_3O_4) carbonaceous absorber materials by electron spectroscopy. Journal of Electron Spectroscopy and Related Phenomena. 2018;229 47–51. Available:https://doi.org/10.1016/j.elspec.2018.09.008
28. Chen B, Chen Z. Sorption of naphthalene and 1-naphthol by biochars of orange peels with different pyrolytic temperatures. Chemosphere. 2009;76(1):127–133. Available:https://doi.org/10.1016/j.chemosphere.2009.02.004
29. Mukome FND, Zhang X, Silva LCR, Six J, Parikh SJ. Use of chemical and physical characteristics to investigate trends in biochar feedstocks. Journal of Agricultural and Food Chemistry. 2013;61(9):2196–2204. Available:https://doi.org/10.1021/jf3049142
30. Wang Z, Zheng H, Luo Y, Deng X, Herbert S, Xing B. Characterization and in fl uence of biochars on nitrous oxide emission from agricultural soil. Environmental Pollution, 2013;174:289–296. Available:https://doi.org/10.1016/j.envpol.2012.12.003
31. Jindo K, Matsumoto K, García Izquierdo C, Sonoki T, Sanchez-Monedero MA. Methodological interference of biochar in the determination of extracellular enzyme activities in composting samples. Solid Earth. 2014;5(2):713–719. Available:https://doi.org/10.5194/se-5-713-2014
32. Jindo K, Mizumoto H, Sawada Y, Sanchez-Monedero MA, Sonoki T. Physical and chemical characterization of biochars derived from different agricultural residues. Biogeosciences. 2014;11(23):6613–6621. Available:https://doi.org/10.5194/bg-11-6613-2014
33. Abdullah B, Ilyas S, Tahir D. Nanocomposites Fe/Activated Carbon/PVA for microwave absorber: Synthesis and characterization. Journal of Nanomaterials. 2018. Available:https://doi.org/10.1155/2018/9823263
34. Tahir D, Ilyas S, Abdullah B, Armynah B, Kim K, Kang HJ. Modification in electronic, structural, and magnetic properties based on composition of composites copper (II) oxide (CuO) and carbonaceous material Modi fi cation in

electronic, structural and magnetic properties based on composition of composit. Ii; 2019.
Available:https://doi.org/https://doi.org/10.1016/0922-338X(91)90208-X

35. Takagi H, Maruyama K, Yoshizawa N, Yamada Y, Sato Y. XRD analysis of carbon stacking structure in coal during heat treatment. Fuel. 2004;83(17–18): 2427–2433.
Available:https://doi.org/10.1016/j.fuel.2004.06.019
36. Meng Junqing Li S, Niu J. Crystallite Structure Characteristics and Its Influence on Methane Adsorption for Different Rank Coals. ACS Omega. 2019;4(24):20762–20772.
Available:https://doi.org/10.1021/acsomega.9b03165
37. Nguyen BT, Lehmann J, Hockaday WC, Joseph S, Masiello CA. Temperature sensitivity of black carbon decomposition and oxidation. Environmental Science and Technology, 2010;44(9):3324–3331.
Available:https://doi.org/10.1021/es903016y
38. Lim TJ, Spokas KA, Feyereisen G, Novak JM. Predicting the impact of biochar additions on soil hydraulic properties. Chemosphere. 2016;142:136–144.
Available:https://doi.org/10.1016/j.chemosphere.2015.06.069
39. Ratzke C, Gore J. Modifying and reacting to the environmental pH can drive bacterial interactions. PLoS Biology. 2018;16(3):1–20.
Available:https://doi.org/10.1371/journal.pbio.2004248
40. Claoston N, Samsuri AW, Ahmad Husni MH, Mohd Amran MS. Effects of pyrolysis temperature on the physicochemical properties of empty fruit bunch and rice husk biochars. Waste Management and Research, 2014;32(4):331–339.
Available:https://doi.org/10.1177/0734242X14525822
41. Liu X, Zhang Y, Li Z, Feng R, Zhang Y. Characterization of corncob-derived biochar and pyrolysis kinetics in comparison with corn stalk and sawdust. Bioresource Technology. 2014;170:76–82.
Available:https://doi.org/10.1016/j.biortech.2014.07.077
42. Liu Y, Zhu Y, Liu S, Chen S, Li W, Wang Y. Molecular structure controls on micropore evolution in coal vitrinite during coalification. International Journal of Coal Geology. 2018;199:19–30.
Available:https://doi.org/10.1016/j.coal.2018.09.012
43. Glaser B, Lehmann J, Zech W. Ameliorating physical and chemical properties of highly weathered soils in the tropics with charcoal - A review. Biology and Fertility of Soils. 2002;35(4):219–230.
Available:https://doi.org/10.1007/s00374-002-0466-4
44. Novak JM, Busscher WJ, Laird DL, Ahmedna M, Watts DW, Niandou MAS. Impact of biochar amendment on fertility of a southeastern coastal plain soil. Soil Science, 2009;174(2):105–112.
Available:https://doi.org/10.1097/SS.0b013e3181981d9a
45. Ghani WAWAK, Mohd A, da Silva G, Bachmann RT, Taufiq-Yap YH, Rashid U, Al-Muhtaseb AH. Biochar production from waste rubber-wood-sawdust and its potential use in C sequestration: Chemical and physical characterization. Industrial Crops and Products. 2013;44:18–24.
Available:https://doi.org/10.1016/j.indcrop.2012.10.017
46. Ding W, Dong X, Ime IM, Gao B, Ma LQ. Pyrolytic temperatures impact lead sorption mechanisms by bagasse biochars. Chemosphere. 2014;105, 68–74.
Available:https://doi.org/10.1016/j.chemosphere.2013.12.042
47. Cely P, Gasco G, Paz-Ferreiro J, Mandez A. Agronomic properties of biochars from different manure wastes. J Anal Appl Pyrol. 2015;111:173–182.
Available:http://oa.upm.es/35478/1/INVE_MEM_2015_193679.pdf
48. Tag AT, Duman G, Ucar S, Yanik J. Effects of feedstock type and pyrolysis temperature on potential applications of

biochar. Journal of Analytical and Applied Pyrolysis. 2016;120:200–206. Available:https://doi.org/10.1016/j.jaap.2016.05.006

49. Nartey OD, Zhao B. Biochar preparation, characterization, and adsorptive capacity and its effect on bioavailability of contaminants: An overview. Advances in Materials Science and Engineering; 2014. Available:https://doi.org/10.1155/2014/715398

50. Wiedemeier DB, Abiven S, Hockaday WC, Keiluweit M, Kleber M, Masiello CA, McBeath AV, Nico PS, Pyle LA, Schneider MPW, Smernik RJ, Wiesenberg GLB, Schmidt MWI. Aromaticity and degree of aromatic condensation of char. Organic Geochemistry. 2015;78:135–143. Available:https://doi.org/10.1016/j.orggeochem.2014.10.002

51. Kyotani T. Control of pore structure in carbon. Carbon, 2000;38(2):269–286. Available:https://doi.org/10.1016/S0008-6223(99)00142-6

52. Xu G, Lv Y, Sun J, Shao H, Wei L. Recent advances in biochar applications in agricultural soils: Benefits and environmental implications. Clean - Soil, Air, Water. 2012;40(10):1093–1098. Available:https://doi.org/10.1002/clen.201100738

53. Hammes K, Schmidt MWI. Changes of Biochar in Soil. In: Lehmann J, Joseph S (eds) Biochar for environmental management science and tech- nology 2009;33-43). In J. J. S. Lehmann (Ed.), Biochar for Environmental Management: Science and Technology and Implementation, Earthscan in the UK and USA. 2009;169–178 Available:https://doi.org/doi.org/10.4324/9781849770552.

54. Singh N, Abiven S, Torn MS, Schmidt MWI. Fire-derived organic carbon in soil turns over on a centennial scale. Biogeosciences. 2012;9(8):2847–2857. Available:https://doi.org/10.5194/bg-9-2847-2012

55. Yu J, Zhao Y, Li Y. Utilization of corn cob biochar in a direct carbon fuel cell. Journal of Power Sources, 2014;270:312–317. Available:https://doi.org/10.1016/j.jpowsour.2014.07.125

56. Meng Jun, Wang L, Liu X, Wu J, Brookes PC, Xu J. Physicochemical properties of biochar produced from aerobically composted swine manure and its potential use as an environmental amendment. Bioresource Technology. 2013;142:641–646. Available:https://doi.org/10.1016/j.biortech.2013.05.086

57. Verheijen F, Jeffery S, Bastos A, Velde VD, Diafas I. Biochar Application to Soils A Critical Scientific Review of Effects on Soil Properties, Processes and Functions; 2010. Available:https://doi.org/10.2788/472

58. Feng B, Bhatia SK, Barry JC. Variation of the crystalline structure of coal char during gasification. Energy and Fuels. 2003;17(3):744–754. Available:https://doi.org/10.1021/ef0202541

59. Lempang M, Syafii W, Pari G. Structure and components of charcoal and activated charcoal from candlenut shell. 2011;278–294.

60. Keiluweit M, Nico PS, Johnson MG. Dynamic Molecular Structure of Plant Biomass-Derived Black Carbon (Biochar). 2010;44(4):1247–1253.

61. Hay ID, Rehman ZU, Moradali MF, Wang Y, Rehm BHA. Minireview Microbial alginate production, modification and its applications; 2013 Available:https://doi.org/10.1111/1751-7915.12076

62. Liang B, Lehmann J, Sohi SP, Thies JE, O'Neill B, Trujillo L, Gaunt J, Solomon D., Grossman J, Neves EG, Luizão FJ. Black carbon affects the cycling of non-black carbon in soil. Organic Geochemistry. 2010;41(2):206–213. Available:https://doi.org/10.1016/j.orggeochem.2009.09.007

63. Septianti E, Salengke, Langkong J, Sukendar NK, Hanifa AP. Characteristic quality of pinrang's cocoa beans during fermentation used styrofoam containers. Canrea Journal: Food Technology, Nutritions and Culinary Journal. 2020;3(1):10-25. Available:https://doi.org/10.20956/canrea.v3i1.235